Pergamon

Prog. Biophys. molec. Biol., Vol. 65, No. 2, pp. 251–264, 1996

0079–6107/96 $32.00 + 0.00

PII: S0079–6107(96)00013–2

GRAMICIDIN PERFORATED PATCH RECORDING AND INTRACELLULAR CHLORIDE ACTIVITY IN EXCITABLE CELLS

NORIO AKAIKE

Department of Physiology, Faculty of Medicine, Kyushu University, Fukuoka 812-82, Japan

CONTENTS

I. INTRODUCTION

Recent developments and improvements in the conventional patch-clamp techniques consisting of four variants (whole-cell, cell-attached, inside-out, outside-out modes) have revolutionized the study of membrane physiology (Kostyuk *et al.*, 1975; Lee *et al.*, 1977; Akaike *et al.*, 1978; Hamill *et al.*, 1981). In particular, the whole-cell recording mode has proven to be the most popular, owing to the ease and speed of obtaining and analysing macroscopic currents. However, the dialysis of the intracellular side with a whole-cell pipette filled with artificial solution washes out the cytoplasmic biochemicals, required for channel activities and second messenger-mediated responses, and also disrupts intracellular Ca^{2+} buffering systems. This disadvantage of the conventional whole-cell recording mode was overcome by the advent of the nystatin perforated patch recording configuration (Horn and Marty, 1988). Since the antibiotic nystatin forms small pores in the cell membrane under the patch pipette, and these pores allow such small monovalent ions as Li^+, Na^+, K^+, Cs^+, choline$^+$, (H^+) and Cl^- to pass while preventing the movement of larger molecules such as Mg^{2+}, Ca^{2+}, glucose-6-phosphate dehydrogenase, nicotinamide adenine dinucleotide phosphate ($NADP^+$) and SO_4^{2-} (Cass and Dalmark, 1973; De Kruijff and Demel, 1974; Kleinberg and Finkelstein, 1984). Consequently, the electrical access to the whole cell can be obtained with a minimal dialysis of the cytoplasm, therefore preventing the loss of intact intracellular constituents that occurs in

the conventional whole-cell patch recording mode. As a result, nystatin perforated patch recording configuration could be applied to a number of functional studies of electrically and chemically excitable and non-excitable cells which are modulated by intracellular mechanisms; i.e. voltage-dependent Na^+, K^+ and Ca^{2+} channels, ligand-operated and G-protein-mediated responses, and transport phenomena across such cytoplasmic membranes as Na^+–Ca^{2+} exchange and electrogenic Na^+–K^+ transport (for review see Akaike and Harata, 1994).

Cl^- is one of the major ionic constituents of the cells and extracellular spaces. Intracellular Cl^- plays an important role in regulating the cell volume and pH (Hoffmann and Simonsen, 1989), in both salt secretion and reabsorption (Petersen, 1991), in membrane excitability (Deisz and Lux, 1982), and G-protein-dependent intracellular signal transduction (Higashijima *et al.*, 1987). γ-Aminobutyric acid (GABA) and glycine are the primary inhibitory neurotransmitters throughout the mammalian central nervous system (CNS). Such agonist-stimulated responses are affected by the intracellular Cl^- concentration. However, it is difficult to make an electrical recording of the neuronal responses with the physiological intracellular Cl^- activity (aCl_i) and the measurement of aCl_i in mammalian neurons because of the following technical limitations. The intracellular recording with a glass microelectrode filled with 1.5–3 M KCl is accompanied by the leakage of a high concentration of Cl^- through a slightly damaged electrode tip and thus easily injures small mammalian CNS neurons. The tip diameter of a Cl^--sensitive electrode is also too large for small CNS neurons to tolerate. Even the recently developed nystatin perforated patch technique suffered from aCl_i disruption because the antibiotic ionophore nystatin allows the permeation of not only monovalent cations but also Cl^- (Marty and Finkelstein, 1975; Horn and Marty, 1988). In addition, the Cl^- in the pipette solution containing nystatin can diffuse into the cell interior, whereas most intracellular anions are immobile because of their high molecular weight, producing a Donnan equilibrium across the nystatin perforated patch membrane. The resulting junctional potential has been reported to be about 9 mV, depending on the recording conditions, which hinders the analysis of the voltage-dependent properties of ionic channels (Akaike and Harata, 1994; Horn and Marty, 1988). As a result, previous studies have been conducted in non-physiological gradients of Cl^- across the cell membrane. Recently, this difficulty was overcome by developing a new perforated patch recording mode using gramicidin in our laboratory (Abe *et al.*, 1994; Rhee *et al.*, 1994; Ebihara *et al.*, 1995; Tajima *et al.*, 1996). Gramicidin is a polypeptide antibiotic that forms pores in the cell membrane as well as nystatin but allows only monovalent cations to permeate the membrane (Hladky and Haydon, 1972) with the result that both aCl_i and the second messenger system remain relatively undisturbed.

In this study we would like to primarily focus on the GABA- and glycine-induced Cl^- responses in mammalian CNS neurons maintaining physiologically intact intracellular Cl^- concentrations by the use of a gramicidin perforated patch recording configuration and thus estimate the aCl_i from the reversal potential of these agonist responses.

II. GRAMICIDIN-FORMED PORES IN THE NATIVE CELL MEMBRANE

2.1. *Gramicidin Solution*

The gramicidin D, used in the present study, is a mixture of gramicidin A, B, and C (Sawyer *et al.*, 1990), which are reported to form structurally equivalent ion channels. The solution of gramicidin D (Sigma) is prepared by dissolving gramicidin in methanol at 10 mg/ml; we usually dissolve 1–2 mg of gramicidin in 100–200 μl. After ultrasonication for 10 sec, the transparent stock solution is directly dissolved in the pipette solution without any pH adjustment just before use, resulting in a final concentration of 0.1 mg/ml. Since the pipette solution with gramicidin loses its activity within 2 hr, we frequently prepared the gramicidin pipette solution during the experiments. When gramicidin acts once as a channel-forming ionophore on the patch cell membrane within 2 hr, the ion-

conducting channels are maintained for at least 3–4 hr. In addition, the final concentration of methanol in the pipette (internal) solution in the absence of gramicidin had no obvious effects on the CNS neurons and cardiac myocytes used.

The standard pipette (internal) solution has the following composition (in mM): KCl, 150; and *N*-2-hydroxyethylpiperazine-*N'*-2-ethanesulfonic acid (HEPES), 10. The pH of the internal solution is adjusted to 7.2 with Tris(hydroxymethyl)aminomethane (Tris-OH). The ionic compositions of external and internal solutions should be further modified for the experimental purposes and different preparations used.

2.2. *Patch Pipettes*

Patch pipettes are fabricated from thick Pyrex glass tubes (1.5 mm outer diameter, 0.9 mm internal diameter, without filament; Narishige, G-1.5) in two stages on a vertical pipette puller. The electrode tip has an internal diameter of 1–2 μm for small CNS neurons. The pipette resistance is 5–8 MΩ. The gramicidin-containing solution is filled to the tip, which has no deleterious effect on the GΩ seal. When patch pipettes with a larger internal diameter (3–5 μm) are used for larger cells such as cerebellar Purkinje cells and cardiac myocytes, gramicidin easily diffuses out from the pipette tip and interferes with seal formation. In such cases, the pipette tips are initially filled with gramicidin-free internal solution by brief immersion. The remainder of the pipette is then back-filled with the same solution containing gramicidin. Mixing was initiated just prior to inserting the patch pipette electrode in the holder, by tapping the electrode to remove any air bubbles at the interface between the two solutions.

2.3. *Getting the Patch*

2.3.1. *Dissociated cardiac myocytes*

The pipette solution contained 150 mM KCl and 0.1 mg/ml gramicidin D. After the GΩ seal was obtained (at time 0 in Fig. 1), the holding potential (V_H) was set up to −40 mV, and a 20-msec hyperpolarizing pulse to −50 mV was applied every 10 sec.

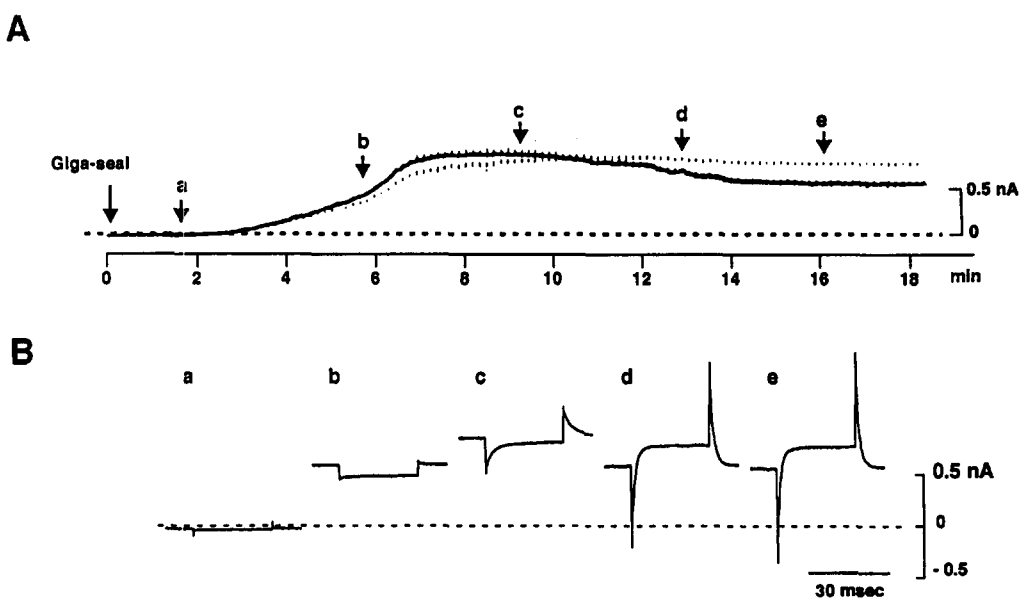

Fig. 1. Time-course for the membrane perforation of dissociated guinea pig cardiac myocytes induced by gramicidin. A: The original recording on a chart recorder. After a gigaohm (GΩ) seal was established (at time 0), pipette potential (holding potential, V_H) was set at −40 mV, and a hyperpolarizing pulse of 10-mV amplitude with 20-msec duration was repeated at 0.1 Hz. Pipette (internal) solution contained 150 mM KCl and 0.1 mg/ml gramicidin D. B: The current responses to pulses at the times indicated by corresponding letters (a–e) in A on an expanded time-scale. Dashed line, zero-current level. From Tajima *et al.*, 1996 with permission.

Under these conditions, the holding current, which was initially zero, gradually shifted to an outward direction. The change in the holding current was accompanied by the appearance of the capacitive charge in response to the voltage pulses, which indicated a time-dependent spontaneous perforation of the patch membrane in the presence of gramicidin. The decay of the capacitive current was gradually accelerated and then became stable at about 16 min after the formation of the GΩ seal.

The time-course of the membrane perforation was quantitatively analysed by measuring the decay time of the capacitive current. Figure 2, inset, shows an example, where the decay time-course closely matched the single-exponential function with a time constant (τ) of 1.2 msec. The measured time constant is plotted against the time, in which the time constant became stable at about 16 min after the formation of a GΩ seal. Regarding an average of 12 cells, the time constant was 1.29 ± 0.44 msec at 16 min. With the assumption that the time constant is given simply by a product of the access resistance (*Ra*) and the membrane capacitance, the value of *Ra* was 9.2 ± 1.5 MΩ at 16 min.

The concentration-dependent effect of gramicidin in the pipette solution was investigated by varying concentrations. At a concentration of 0.1 mg/ml gramicidin, membrane perforation was achieved on all 12 patches; however, a weaker concentration decreased the success rate of the membrane perforation. In five of 13 patches and in five of 10 patches in which the gramicidin concentration was 0.01 and 0.001 mg/ml, respectively,

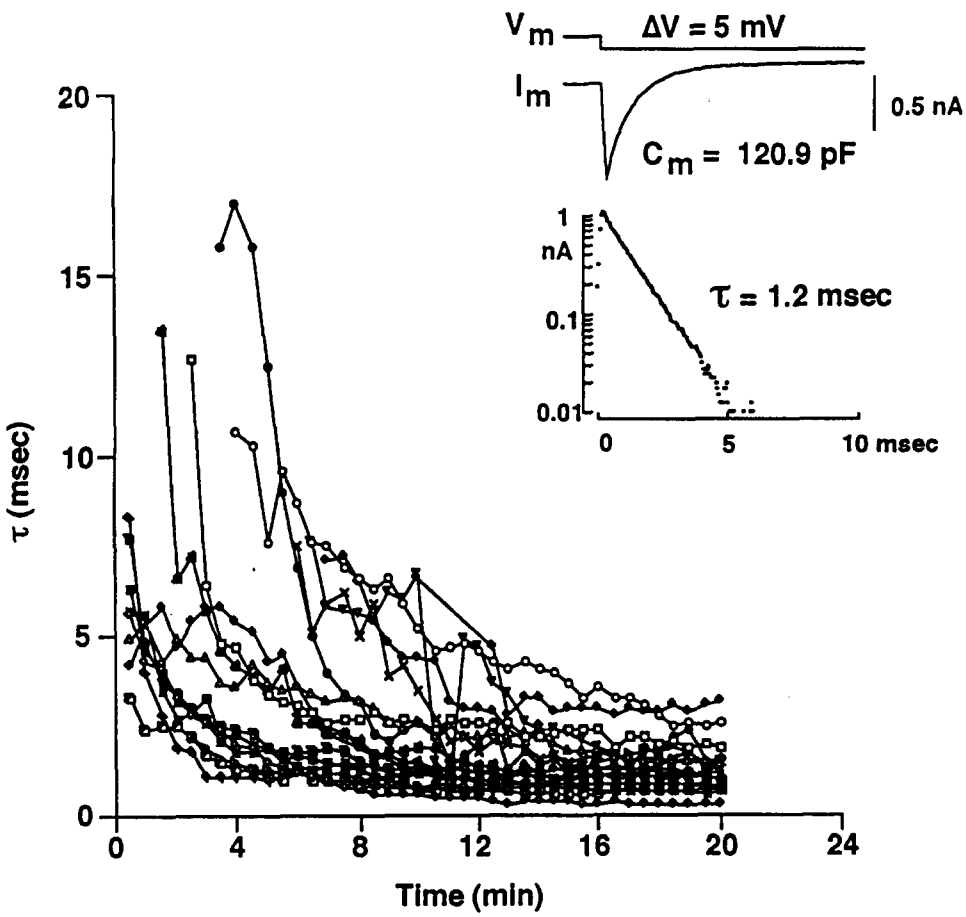

Fig. 2. Measurement of the time constant during the perforation of guinea pig cardiac myocyte membrane by 0.1 mg/ml gramicidin. Time constant (τ) plotted against experimental time. The data from 12 cells are shown, and different symbols indicate different cells. *Inset*: capacitive current recorded during perforation of patch membrane (*top*) and on a semilogarithmic scale (*bottom*). The least-squares fit to decay phase gives a value of 1.2 msec. V_m, membrane potential; ΔV, change in potential; I_m, membrane current; C_m, membrane capacitance. From Tajima *et al.*, 1996 with permission.

we failed to detect any obvious membrane perforation during >20 min after the GΩ seal. *Ra* was thus measured in the successfully perforated patches at 20 min after formation of the GΩ seal. A concentration >0.1 mg/ml might further facilitate membrane perforation. However, no such trials were attempted in this study, because the possible side effects of methanol used as a solvent could not be completely ruled out. As a result, a gramicidin concentration of 0.1 mg/ml seemed to be optimal to obtain a successful perforation, and therefore this concentration was used in most of our experiments.

2.3.2. *Dissociated CNS neurons*

When the patch pipette containing 0.1 mg/ml gramicidin was applied on the dissociated rat substantia nigra pars reticulata (SNR) neurons, the time-dependent development of the capacitive current was also observed (Ebihara *et al.*, 1995). After 35–40 min, both the peak amplitude and the kinetics of capacitive current became constant, the constant capacitive current remained for the following 2 hr, thus indicating that the density of the gramicidin pores formed in the patch membrane was stable. The capacitive current usually reached more than 500 pA and the *Ra* dropped to less than 20 MΩ within 35–40 min after making the GΩ seal. The mean minimum *Ra* was 16.1 ± 1.2 MΩ ($n=8$) during a 2-hr observation. The current measurements were started after the stabilization of the capacitative current in neurons having a resting membrane potential more negative than −45 mV. The mean input capacitance was 15.6 ± 2.6 pF ($n=5$), which was comparable to the 17.2 ± 1.8 pF ($n=5$) obtained by the conventional whole-cell patch recording mode.

In the dissociated rat CNS neurons (Abe *et al.*, 1994; Rhee *et al.*, 1994; Ebihara *et al.*, 1995), the membrane perforation required >30 min after the GΩ seal was established, whereas about 16 min was required in the dissociated guinea pig ventricular cells (Tajima *et al.*, 1996). This difference might be attributable to the different experimental conditions between the two studies. The experiments using brain cells were carried out at room temperature (22–24°C) and the resistance of the patch pipettes ranged from 4 to 6 MΩ. A relatively large pipette (1.5–3 MΩ) and high temperature (35.5°C) might have facilitated the incorporation of gramicidin into the cardiac cell membrane.

2.4. *Cation Selectivity of Gramicidin Perforated Cell Membrane*

To examine the ion selectivity of the gramicidin perforated channels in the native cell membrane, a cell-free patch from the dissociated guinea pig ventricles was obtained after confirmation of the membrane perforation. The pipette solution contained 150 mM KCl. The holding potential (V_H) was set at 0 mV, and the square pulses of 300 msec were applied from −50 to +50 mV in 10-mV increments. Figure 3 shows typical records obtained with various test bath solutions (intracellular side): 150 mM KCl, Tris-Cl, K-aspartate, NaCl and CsCl. The upward deflection indicates the current flow from the intracellular side (bath) toward the pipette side (outward current) and vice versa. With the 150 mM KCl bath solution, the holding current was almost zero, whereas the depolarizing and hyperpolarizing pulses produced symmetrical current shapes, as expected from the symmetrical ionic compositions. With the Tris-Cl solution, however, the holding current was inward, and no obvious outward current was seen at the end of the pulse. On the other hand, the symmetrical current shape was well conserved with the K-aspartate solution, thus indicating the current to be largely carried by K^+, and not by Cl^-. The outward current, which could largely reflect an outward flux of cations in the bathing solution, was larger in the CsCl solution and smaller in the NaCl solution than in the KCl solution. A slight decay was also observed during the depolarizing or hyperpolarizing voltage pulses as shown in Fig. 3. The extent of the decay varied from patch to patch; i.e., in some cells the current showed a decay such as Fig. 3, whereas no time-dependent change was detected in others. Therefore, it is not likely that the gramicidin channels acquired any voltage-dependent properties in the native cell membrane. Thus, the current decay seen in Fig. 3 might be due to an accumulation or depletion of the permeating cations in the unstirred layer of the patch membrane.

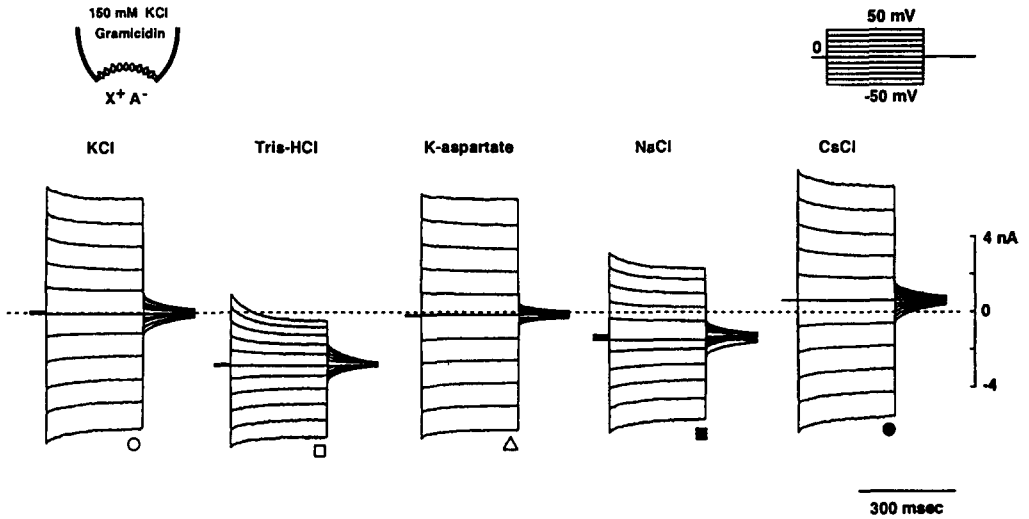

Fig. 3. Monovalent cation-selective nature of gramicidin channels in cardiac cell membrane. After membrane perforation was confirmed by gramicidin, the cell-free patch was obtained. Current records in response to the pulse protocol (*top*) are superimposed, and a downward deflection indicates a current flow from the pipette toward the bath. The main composition of bathing medium is indicated above each trace. Dashed line, zero-current level. From Tajima *et al.*, 1996 with permission.

When the ionic permeability of the gramicidin perforated channels was calculated by the Goldman–Hodgkin–Katz equation using the reversal potentials obtained from the current–voltage relationships in each ion solution, the monovalent cation permeability relative to K^+ (P_X/P_K) was 0.64 for Na^+, 1.11 for Cs^+, and 0.1 for $Tris^+$. Regarding the quantitative aspect, however, the value of the permeability seems to be slightly different between the artificial membrane and the native cell membrane; i.e., in the artificial lipid bilayers, P_{Cs}/P_K and P_{Na}/P_K were reported to be about 1.3 and 0.3, respectively (Myers and Haydon, 1972). The difference can thus be explained by assuming different compositions of the lipid bilayers between the two membranes. In fact, it is well known that the permeability characteristics of gramicidin channels depend on the composition of phospholipids of the bilayers (Andersen, 1984). In general, however, the relative order of cation selectivity obtained in the cardiac cells is in good accordance with the selective sequence established in the lipid bilayers ($H^+ > NH_4^+ > Cs^+ > Rb^+ > K^+ > Na^+ > Li^+$) (Hille, 1992; Myers and Haydon, 1972). In addition, Cl^- permeability could not be detected in the artificial membrane (Myers and Haydon, 1972) or in the present native cell membrane, which confirmed that the gramicidin channel is highly selective for small monovalent cations.

III. APPLICATIONS OF GRAMICIDIN PERFORATED PATCH

Gramicidin has now been applied to both electrically and chemically excitable cells. Below, we will review some of the reported applications of the gramicidin perforated patch recording mode.

3.1. *Action Potential and Membrane Current*

The resting potential of guinea pig ventricle muscles under current-clamp conditions measured by gramicidin perforated patch recording mode was -84.2 ± 1.2 mV ($n=23$). The amplitude and duration of the action potential were 128.6 ± 3.3 mV and 173.1 ± 31.3 msec ($n=9$), respectively (Fig. 4A). These values were in good agreement with those reported in the previous study (Isenberg and Klockner, 1982).

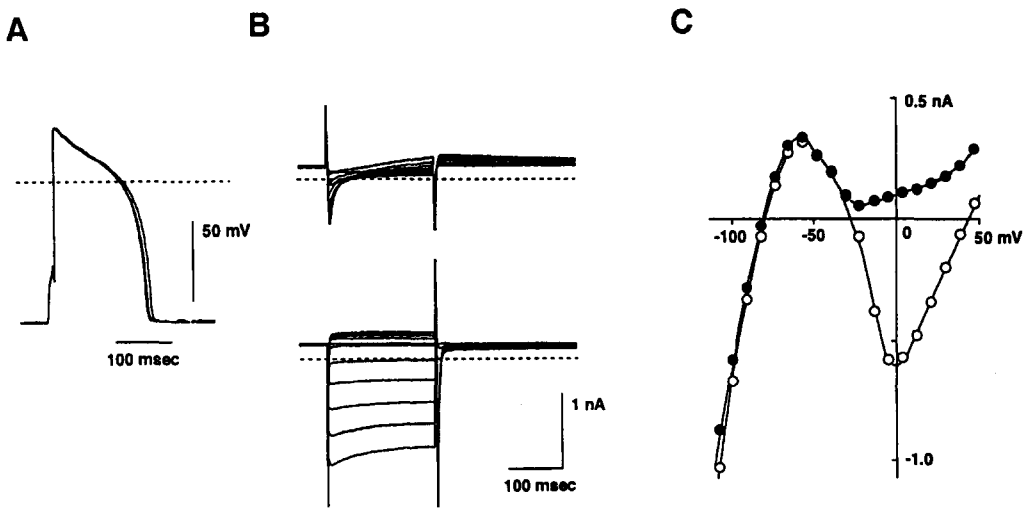

Fig. 4. The action potential and whole cell currents in the guinea pig ventricular cells by the gramicidin perforated patch recording mode. A: Action potential recorded in current-clamp conditions. Dashed line, zero-potential level. Pipette contained 150 mM KCl and 0.1 mg/ml gramicidin. B: Membrane currents, elicited by various test pulses more positive than −40 mV (*top*) under voltage-clamp condition and those at more negative potentials (*bottom*), are superimposed. Pulse duration is 200 msec; dashed lines, zero-current level. C: Current–voltage relationships measured at peak (○) and just before end of pulse (●). The smooth curves were drawn by eye. From Tajima *et al.*, 1996 with permission.

The intactness of the electrophysiological properties was confirmed by recording the membrane currents under voltage-clamp conditions. The depolarization of the membrane from a V_H to various potentials activated a Ca^{2+} current, which was followed by a gradual development of the delayed rectifier K^+ current (Fig. 4B, top). Regarding hyperpolarization, an instantaneous jump of the current due to the inward rectifier K^+ current was also observed (Fig. 4B, bottom). A typical N-shaped curve was observed in the steady-state current–voltage relationship, and the amplitude of the inward Ca^{2+} current also showed a peak at about 0 mV (Fig. 4C). Figure 5 shows the amplitude of the voltage-dependent Ca^{2+} current which remained almost constant during a continuous recording of more than 80 min by the gramicidin perforated patch recording mode. The peak inward current at 0 mV was 97.8% of the control even after 1 hr from the start of recording, thus indicating that gramicidin perforated patch recording is effective for measuring the ionic currents with little rundown of the currents in a similar way to nystatin or amphotericin B perforated patch recording. These findings also support the validity of using gramicidin as a tool for the perforated patch recording.

3.2. *GABA Response*

The CNS neurons possess several types of Cl^--selective channels. Intracellular Cl^- concentration ($[Cl^-]_i$) is not constant among neurons depending on certain factors; i.e. active Cl^- transport, passive membrane properties and developmental stages (Misgeld *et al.*, 1986; Cherubini *et al.*, 1991). Such variability may determine the functional consequences of Cl^- channel activation. Since the CNS neurons of adult mammals have generally low $[Cl^-]_i$ and high extracellular Cl^- ($[Cl^-]_o$), the activation of $GABA_A$ receptors usually induces hyperpolarization, or at least a shunting of the excitatory postsynaptic potentials, resulting in the observed inhibition.

3.2.1. *GABA response and intracellular Cl^-* activity (aCl_i)

Under the current-clamp conditions of the gramicidin perforated patch recording mode with the external solution containing 161 mM Cl^- and the patch pipette (internal) solution containing 150 mM Cl^-, 10^{-5} M GABA hyperpolarized the acutely dissociated

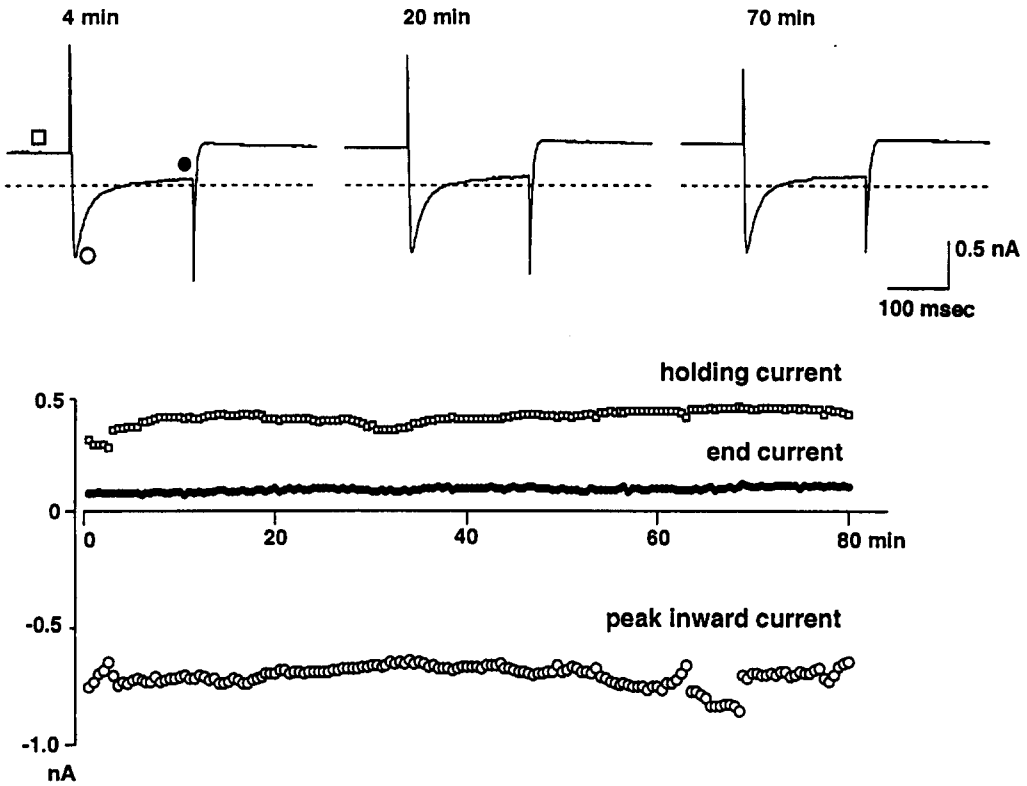

Fig. 5. Time-course of voltage-dependent Ca^{2+} current in guinea pig cardiac cell recorded by gramicidin perforated patch recording configuration over 80 min. A voltage pulse of 200-msec duration and 40-mV amplitude was repeated at 0.1 Hz at a V_H of −40 mV. *Top*: original current traces recorded at the times indicated above each trace. Dashed lines, zero-current level. *Bottom*: the amplitudes of the holding current (□), peak inward current (○), and current just before end of pulse (●) plotted against experimental time. From Tajima *et al.*, 1996 with permission.

rat substantia nigra pars reticulata (SNR) neuron having a resting potential of −58 mV and inhibited the spontaneous firings (Fig. 6A). When the GABA was applied to the same neuron at a V_H of −50 mV, an outward current was observed (Fig. 6B). At 5 min after rupturing the patch membrane by applying greater negative pressure to the same patch pipette interior, GABA induced an inward current at the same V_H (Fig. 6C). The polarity of GABA-induced currents differed dramatically between the gramicidin perforated patch recording and the conventional whole-cell patch recording modes in the same neuron. These results also confirm that Cl^- can not pass the gramicidin-formed cation-selective channels.

To know the intact aCl_i in the dissociated rat SNR neurons, the gramicidin perforated patch recording mode was used (Ebihara *et al.*, 1995). This method could give a relatively accurate measurement of the GABA-gated Cl^- reversal potential (E_{GABA}). In the 40 SNR neurons perfused with external solution with 161 mM Cl^-, the E_{GABA} measured from current–voltage relationships ranged between −94.0 and −44.9 mV (Fig. 7A). Figure 7B shows the distribution histogram of aCl_i calculated by the Nernst equation using both the extracellular Cl^- activity (aCl_o) and E_{GABA} values. The aCl_i ranged from 2.8 to 19.7 mM with a mean value of 9.5 ± 0.7 mM ($n = 40$). When the E_{GABA} values in five neurons were measured again 1 hr after the first measurement, there was no significant change, thus indicating that the aCl_i of individual neurons was well maintained and that the gramicidin-formed pores are not permeable to Cl^- even in the presence of larger amounts of Cl^- (150 mM) in the recording patch pipette solution.

When the E_{GABA} was measured in the SNR neurons by three other patch techniques such as conventional whole-cell, nystatin perforated and amphotericin B perforated patch

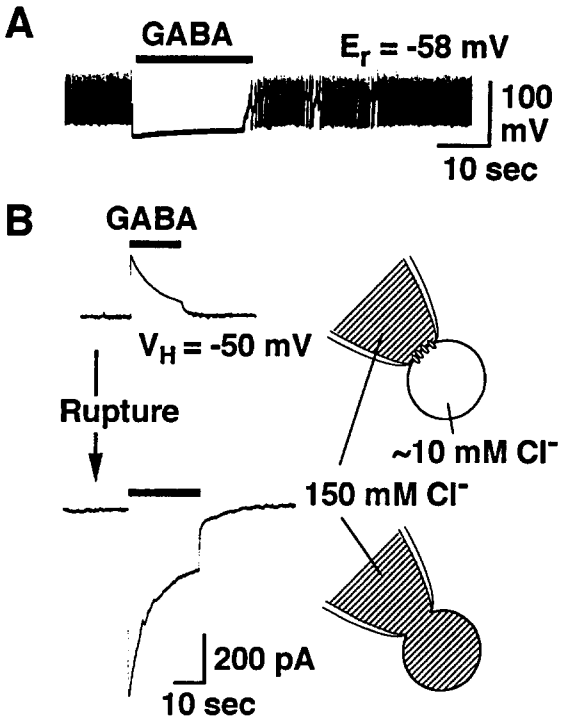

Fig. 6. Gramicidin perforated patch recording from dissociated rat substantia nigra pars reticulata (SNR) neurons. A: Current-clamp recording of the membrane potentials. 10^{-5} M GABA was applied during the period indicated by a horizontal bar. The resting potential (E_r) was −58 mV. B: GABA-induced outward and inward currents at a V_H of −50 mV before and after the rupture of patch membrane, respectively. *Upper panel*: In this condition, the intracellular Cl^- concentration was not disturbed by the Cl^- present in the patch pipette solution (shown schematically at right of the current trace). *Lower panel*: GABA-induced inward current after a rupture of the patch membrane in the same neuron. In this case, the patch pipette Cl^- completely diffused into the cell within 5 min of the rupture and the intracellular Cl^- concentration reached 150 mM, the same concentration as in the pipette solution (shown schematically at right). From Ebihara *et al.*, 1995 with permission.

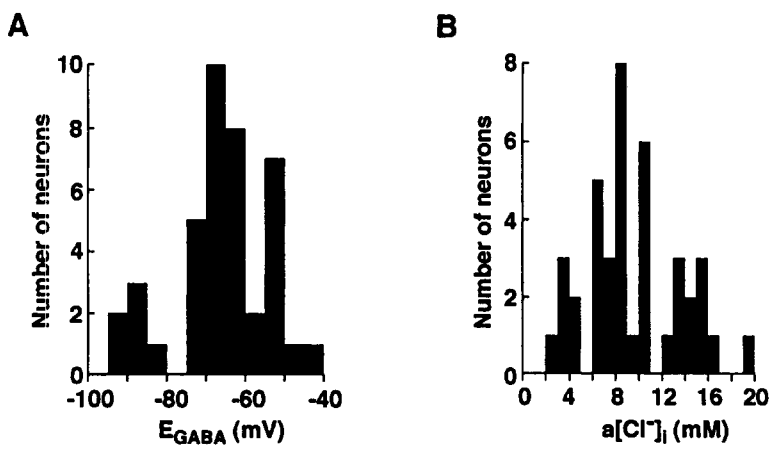

Fig. 7. Distributions of the reversal potential (E_{GABA}) of GABA-induced currents and intracellular Cl^- activities (aCl_i) in dissociated rat SNR neurons obtained by the gramicidin perforated patch recording mode. A: Histogram shows the distribution of E_{GABA} of 40 neurons. B: Histogram indicates the distribution of aCl_i calculated with the Nernst equation using data in A. From Ebihara *et al.*, 1995 with permission.

recording modes, these techniques yielded the E_{GABA} values of -2.2 mV ($n=5$), -2.5 mV ($n=5$) and -3.0 mV ($n=4$), respectively, with no statistically significant differences among them. These E_{GABA} values were close to the Cl^- equilibrium potential (E_{Cl}) of -1.7 mV calculated with the Nernst equation. Since pipette solution for the four modes including gramicidin perforated patch recording was exactly the same, these results indicate that aCl_i is maintained intact in the gramicidin method, but is completely disrupted by the pipette solutions of the conventional whole-cell, nystatin perforated and amphotericin B perforated patch recording configurations.

3.2.2. *Developmental changes in the cultured neurons*

When the neurons dissociated from the embryonic day 15 rat hypothalamus were cultured for 1–14 days, the applicaion of GABA depolarized and evoked action potentials in these young cultured neurons. Such a depolarizing effect of GABA in young cultures changed to a hyperpolarizing effect after three weeks of culture (20–33 days) (Fig. 8A, B). Both depolarization in young neurons and hyperpolarization in older neurons induced by GABA were completely antagonized by the addition of bicuculline, a specific blocker of $GABA_A$ receptors (Fig. 8C, D), indicating that both responses occurred through the activation of $GABA_A$ receptors (Chen *et al.*, 1996). Similarly, the GABA-induced response shifted negatively from depolarizing to hyperpolarizing in developing the cultured rat spinal cord dorsal horn neurons (Kyrozis and Reichling, 1995).

3.2.3. *Age-related changes*

The nucleus basalis of Meynert is populated by large cholinergic neurons and is a major source of cholinergic input to cerebral cortex. The Meynert neurons receive GABAergic fibers, and recent molecular biological and pharmacological studies have also revealed the existence of multiple kinds of $GABA_A$ receptor subtypes which differ both during development and in the brain region, though less is known about the functional meanings of the developmental differences. The functional and developmental changes in $GABA_A$ response were thus studied in the acutely dissociated rat Meynert neurons. The whole-cell GABA responses displayed a greater efficacy in the order of 0–2-day- > 6-month- > 2-week-old rat neurons followed by the changes of the GABA receptor affinity and cooperativity. The E_{GABA} became more negative with aging, the aCl_i calculated from the Nernst equation using both aCl_o and E_{GABA} ranged with the mean value of 34.8, 22.3 and 13.1 mM for 0-day-, 2-week- and 6-month-old neurons, respectively (Akaike *et al.*, 1996).

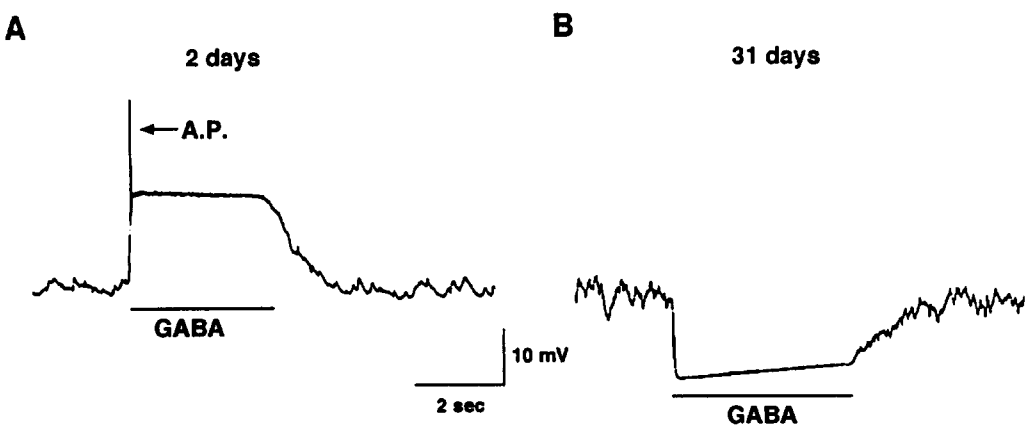

Fig. 8. Developmental change in the GABA response in the cultured rat hypothalamic neurons measured by the gramicidin perforated patch recording mode. A: Action potential (A.P.) and depolarization in young neurons (2 days cultured) in the presence of 3×10^{-5} M GABA. B: GABA-induced hyperpolarization in older neurons (31 days cultured). All the initial membrane potentials were current-clamped at -60 ± 2 mV. The action potential is truncated. From Chen *et al.*, 1996 with permission.

3.2.4. *Effect of neuronal trauma*

When the embryonic day 18 rat hypothalamic neurons were cultured for 24–35 days and the neurons were traumatized by a neurite transection, replating, osmotic imbalance and excess heat, GABA, both synaptically released and exogenously applied, depolarized the neurons (Fig. 9) and increased intracellular Ca^{2+} concentration (van den Pol *et al.*, 1996). The depolarizing actions of GABA after trauma lasted longer than a week.

3.3. *Glycine Response*

Glycine is also an established inhibitory neurotransmitter in the mammalian spinal cord and brain stem. The hyperpolarizing action of glycine in mature animals results from the opening Cl^- channels (Akaike and Kaneda, 1989). However, glycine as well as GABA may depolarize many types of brain cells in the early developmental stages. For example, the glycine response of the rat CA3 neurons shifted from depolarization to hyperpolarization because of a possible modification of Cl^- gradient across the cell membrane during development (Ito and Cherubini, 1991). To study phenomena where aCl_i is an important variable, therefore, it would thus be useful to use the gramicidin perforated patch technique that interferes as little as possible with aCl_i.

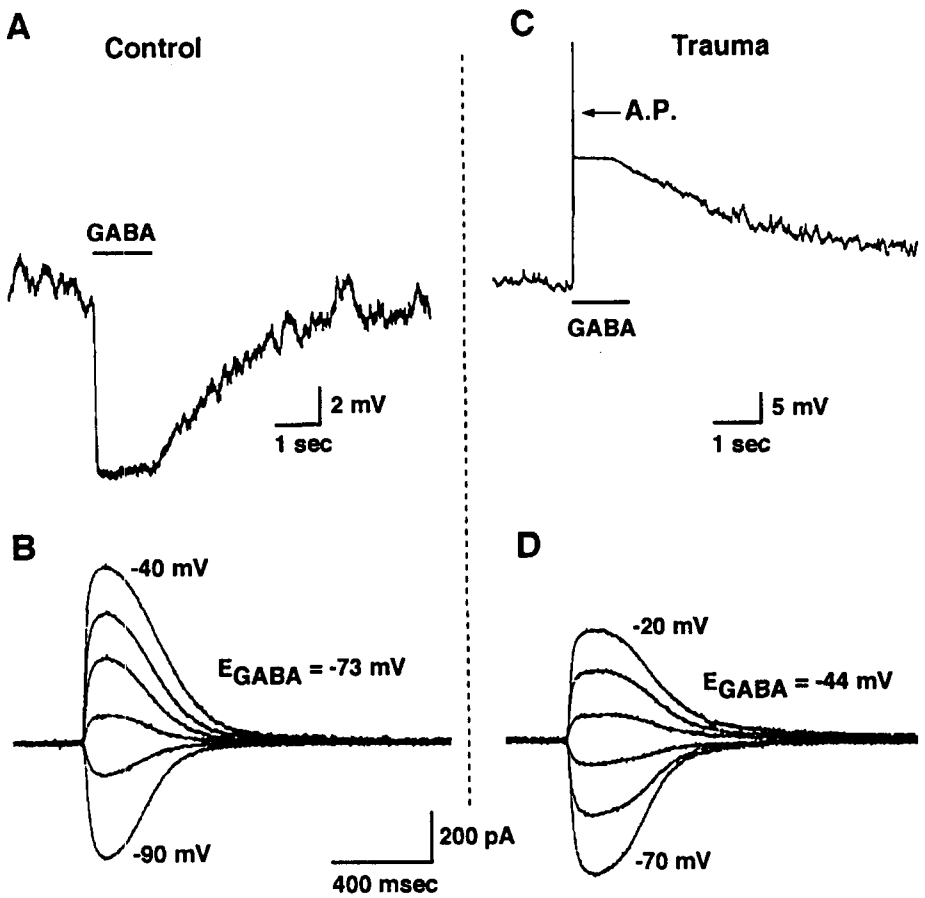

Fig. 9. GABA depolarizes cultured rat hypothalamic neurons after trauma. A and B, control neurons. C and D, traumatized neurons. A: GABA (10^{-5} M) induced a hyperpolarization from −60 to −72 mV in a typical control neuron cultured for 33 days. C: GABA depolarized the neuronal membrane potential from −60 to −38 mV, generating an action potential (A.P.) in a representative traumatized neuron (2 days after replating the 33-day-old cultured neurons). B and D: The reversal potential of GABA-evoked currents determined by gramicidin perforated patch recording mode shifted positively after trauma. The V_H was −60 mV. The command potential was increased by 10 mV steps, and then GABA was applied briefly to determine its reversal potential. From van den Pol *et al.*, 1996 with permission.

Glycine, when microinjected into the nucleus tractus solitarius (NTS) region, elicits decreases in arterial pressure and heart rate (Talman *et al.*, 1991). These cardiovascular responses for glycine were abolished by a specific blocker of glycine receptors, strychnine (Talman and Robertson, 1989), indicating the existence of a glycine receptor on NTS neurons. Using the gramicidin perforated patch recording mode, glycine evoked an outward current in the NTS neurons acutely dissociated from two-week-old rats at a V_H of -45 mV and the response increased in a concentration-dependent manner (Rhee *et al.*, 1994). In contrast, the glycine response recorded by the nystatin perforated patch recording mode was an inward current. In these experiments, the patch pipette contained 150 mM Cl^-. In the concentration–response relationships, the half-maximum effective concentration (EC_{50}) and the Hill coefficient were 4.0×10^{-5} M and 1.5 for the gramicidin perforated patch recording mode, and 4.9×10^{-5} M and 1.2 for the nystatin perforated patch recording mode. These results indicate that the gramicidin method is comparable to the nystatin method but that the use of gramicidin directly reflects the glycine response in the neurons maintaining physiological aCl_i. Since the glycine-induced current is carried by Cl^-, and the reversal potential (E_{Gly}) of the glycine-induced current is the same as the Cl^- equilibrium potential (E_{Cl}), the intact aCl_i could thus be calculated from the Nernst equation knowing aCl_o of 161 mM and E_{Gly} measured by gramicidin perforated patch recording mode. The value of E_{Gly} in NTS neurons ranged from -70.2 to -47.5 mV. The calculated aCl_i value ranged from 7.3 to 18.2 mM, with a mean value of 13.3 mM ($n=29$). In addition, the physiological aCl_i in the ventromedial hypothalamic (VMH) neurons acutely dissociated from eight- to 12-day-old rats, determined by gramicidin perforated patch recording mode, ranged from 6.0 to 43.8 mM ($n=28$) (Abe *et al.*, 1994). There was also a wide distribution of aCl_i between the different preparations. These results also indicate that aCl_i in NTS neurons is low enough to produce glycine-induced inhibitory postsynaptic potential.

Developmental changes in the glycine responses from depolarization to hyperpolarization were also clearly shown in the cultured rat spinal cord dorsal horn neurons by the use of a gramicidin perforated patch recording configuration (Kyrozis and Reichling, 1995). A neuron that was kept for 6 days in culture and recorded with a patch pipette (internal) solution with 6 mM Cl^- was depolarized to -46 mV. Another neuron was kept in a 34-day-old culture and recorded with 50 mM Cl^- in the pipette responded by a hyperpolarization to -75 mV. Since glycine receptor heterogeneity is related to the development of neural plasticity (Schofield *et al.*, 1990), it may also be expected that the shifting of aCl_i might also be related to developing neural plasticity by modifing the neural excitabilities.

3.4. *Odor-induced Response*

Odor transduction in olfactory receptor neurons is a complex process involving more than one second-messenger pathway. The cyclic adenosine-3′,5′-monophosphate (cAMP)-mediated signal transduction cascade in the vertebrate olfactory receptor neurons is well understood (for review see Dionne and Dubin, 1994). When order molecules activated the G-protein-coupled receptor, the intracellular cAMP level is increased, thus resulting in the direct opening of the cation channels. Ca^{2+} ions passing through this channel activate Cl^- current (Ca^{2+}-activated Cl^- current, $I_{Ca(Cl)}$). Such secondary Cl^- currents comprised a significant part of the odor-evoked currents (about 60%) in *Xenopus laevis* olfactory receptor neurons (Zhainazarov and Ache, 1995). The E_{Cl} measured by gramicidin perforated patch recording mode was -2.3 mV, indicating that these neurons maintain a high aCl_i. The estimation of aCl_i from the Nernst equation gave a value of 119 mM, thereby implicating an excitatory role for Cl^- current in olfactory transduction.

3.5. *Catecholamine-induced Response*

It is well known in mammalian cardiac cells that β-adrenergic stimulation activates a Cl^- current via the cAMP-mediated cellular mechanism (Bahinski *et al.*, 1989; Harvey and Hume, 1989). When the catecholamine-induced Cl^- current in single myocytes

acutely dissociated from guinea pig ventricles was recorded by the gramicidin perforated patch recording mode, the reversal potential of Cl^- current was -36.1 ± 2.4 mV ($n = 19$), giving aCl_i of 36.3 ± 2.9 mM (Tajima *et al.*, 1996).

3.6. *Application to Brain Slice Preparation*

The response of a dissociated neuron to exogenous GABA and glycine does not necessarily confirm its role as a natural transmitter. Therefore, slice-patch recordings were made on SNR neurons held at a V_H of -50 mV using the gramicidin perforated patch recording mode. The inhibitory postsynaptic currents (IPSCs) and the excitatory postsynaptic currents (EPSCs) were recorded in different current directions; i.e. the former are outward currents while the latter are inward currents. The spontaneous IPSCs were competitively blocked by bicuculline, indicating that the spontaneous IPSCs are induced by GABA release from the GABAergic nerve terminals to SNR neurons. These findings also indicate that we easily separated GABA- or glycine-mediated IPSCs and EPSCs by holding the membrane at a resting potential. Therefore, the gramicidin technique provides a new possibility for comparative studies of synaptic function and connectivity (Ebihara *et al.*, 1995).

IV. PRECAUTIONS WHEN USING A GRAMICIDIN PERFORATED PATCH

Gramicidin is a linear polypeptide antibiotic that forms voltage-insensitive channels in the cell membranes and transports monovalent cations. The permeability to Cl^- of the gramicidin-formed pores is negligible (Myers and Haydon, 1972), thus giving physicochemical support to the present reports obtained on excitable cells that Cl^- does not move across the gramicidin perforated patch membrane. In contrast, the intracellular cations inevitably move across the membane, and there is the possibility that changes in the intracellular cation concentrations affect the physiological aCl_i. In fact, the existence of a Cl^- transporter involving cations was reported in cultured hippocampal neurons (Inoue *et al.*, 1991). However, the present results suggest that a certain degree of change in intracellular cation concentration does not disturb the intrinsic aCl_i in the dissociated cells. To exclude another possibility that V_H affects the intrinsic aCl_i, we investigated the effects of different V_Hs. Consequently, the intrinsic aCl_i was not affected by the V_Hs between -40 and -100 mV. However, at a V_H of -20 mV, the aCl_i in SNR neurons increased slightly from the control of -60 mV. This may be due to the increase in Cl^- permeability of the neuronal membrane and/or to the dysfunction of the Cl^- pump at higher depolarized membrane potentials.

Although the gramicidin perforated patch recording mode has many advantageous aspects as well as nystatin and amphotericin B perforated patch recording modes, as have been described, the perforation with gramicidin is slower than with nystatin and amphotericin B. The longer time needed for perforation with gramicidin may be related to the fact that two gramicidin molecules, forming a head-to-head dimer, are required for the formation of a functional channel (Hladky and Haydon, 1984).

V. CONCLUSIONS

We have reviewed the experimental aspects of the gramicidin perforated patch recording mode on such excitable cells as neurons, cardiac myocytes and sensory cells. In light of its broad applicability, this technique seems to be of value not only for excitable cells but also for inexcitable cells in studying the functions and modulations of receptors, ion channels and transport phenomena, which are related to both the Cl^--permeable channels and aCl_i regulatory mechanisms. Research on the gramicidin perforated patch recording configuration should thus continue to provide important information relevant to the physiological and pathological conditions of cells.

ACKNOWLEDGEMENTS

We would like to thank Dr. B. Quinn for his critical reading of the manuscript. This work was supported by a Grand-in-Aid for Scientific Research (A) (No. 07407002) and a Grant-in-Aid for Scientific Research on Priority Areas (No. 07276101) from the Ministry of Education, Science and Culture, Japan, to Norio Akaike.

REFERENCES

Abe, Y., Furukawa, K., Itoyama, Y. and Akaike, N. (1994) *J. Neurophysiol.* **72,** 1530–1537.
Akaike, N., Fishman, H. M., Lee, K. S., Moore, L. E. and Brown, A. M. (1978) *Nature* **274,** 379–382.
Akaike, N. and Harata, N. (1994) *Jap. J. Physiol.* **44,** 433–473.
Akaike, N. and Kaneda, M. (1989) *J. Neurophysiol.* **62,** 1400–1409.
Akaike, N., Rhee, J.-S., Jin, Y.-H. and Ono, K. (1996) *GABA: Receptors, Transporters and Metabolism*, pp. 201–207 (eds. C. Tanaka and N. G. Bowery), Birkhauser Verlag, Basel.
Andersen, O. S. (1984) *A. Rev. Physiol.* **46,** 531–548.
Bahinski, A., Nairn, A. C., Greengard, P. and Gadsby, D. (1989 *Nature* **340),** 718–721.
Cass, A. and Dalmark, M. (1973) *Nature* **244,** 47–49.
Chen, G., Trombley, P. Q. and van den Pol, A. N. (1996) *J. Physiol.* **494.2,** 451–464.
Cherubini, E., Gaiarsa, J. L. and Ben-Ari, Y. (1991) *Trends Neurosci.* **14,** 515–519.
De Kruijff, B. and Demel, R. A. (1974) *Biochim. biophys. Acta* **339,** 57–70.
Deisz, R. A. and Lux, H. D. (1982) *J. Physiol.* **326,** 123–138.
Dionne, V. E. and Dubin, A. E. (1994) *J. exp. Biol.* **194,** 1–21.
Ebihara, S., Shirato, K., Harata, N. and Akaike, N. (1995) *J. Physiol.* **484.1,** 77–86.
Hamill, O. P., Marty, A., Neher, E., Sakmann, B. and Sigworth, F. J. (1981) *Pflügers Arch.* **391,** 85–100.
Harvey, R. D. and Hume, R. (1989) *Science* **244,** 983–985.
Higashijima, T., Ferguson, K. M. and Sternweis, P. C. (1987) *J. biol. Chem.* **262,** 3597–3602.
Hille, B. (1992) *Ionic Channels of Excitable Membranes*, 2nd edn., pp. 305–312. Sinauer, Sunderland, MA.
Hladky, S. B. and Haydon, D. A. (1972) *Biochem. biophys. Acta* **274,** 294–312.
Hladky, S. B. and Haydon, D. A. (1984) *Curr. Topics Membr. Transp.* **21,** 327–372.
Hoffmann, E. K. and Simonsen, L. O. (1989) *Physiol. Rev.* **69,** 315–382.
Horn, R. and Marty, A. (1988) *J. gen. Physiol.* **92,** 145–159.
Inoue, M., Hara, M., Zeng, X., Hirose, T., Ohnishi, S., Yasukura, T., Uriu, T., Omori, K., Minato, A. and Inagaki, C. (1991) *Neurosci. Lett.* **134,** 75–78.
Isenberg, G. and Klockner, U. (1982) *Pflügers Arch.* **395,** 19–29.
Ito, S. and Cherubini, E. (1991) *J. Physiol.* **440,** 67–83.
Kleinberg, M. E. and Finkelstein, A. (1984) *J. Membrane Biol.* **80,** 257–269.
Kostyuk, P. G., Krishtal, O. A. and Pidoplichko, V. I. (1975) *Nature* **257,** 691–693.
Kyrozis, A. and Reichling, D. B. (1995) *J. Neurosci. Meth.* **57,** 27–35.
Lee, K. S., Akaike, N. and Brown, A. M. (1977) *Nature* **265,** 751–753.
Marty, A. and Finkelstein, A. (1975) *J. gen. Physiol.* **95,** 515–526.
Misgeld, U., Deisz, R., Dodt, H. and Lux, H. (1986) *Science* **232,** 1413–1415.
Myers, V. B. and Haydon, D. A. (1972) *Biochem. biophys. Acta* **274,** 313–322.
Petersen, O. H. (1991) *J. Physiol.* **448,** 1–51.
Rhee, J.-S., Ebihara, S. and Akaike, N. (1994) *J. Neurophysiol.* **72,** 1103–1108.
Sawyer, D., Williams, L. P., Whaley, W. I.Jr.II, Koeppe, R. E. and Andersen, O. S. (1990) *Biophys. J.* **58,** 1207–1212.
Schofield, P. R., Shivers, B. D. and Seeburg, P. H. (1990) *Trends Neurosci.* **13,** 8–11.
Tajima, Y., Ono, K. and Akaike, N. (1996) *Am. J. Physiol.* **271,** C524–C532.
Talman, W. T., Colling, K. J. E. and Robertson, S. C. (1991) *Am. J. Physiol.* **260,** H1326–H1331.
Talman, W. T. and Robertson, S. C. (1989) *Brain Res.* **477,** 7–13.
van den Pol, A. N., Obrietan, K. and Chen, G. (1996) *J. Neurosci.* **16,** 4283–4292.
Zhainazarov, A. B. and Ache, B. W. (1995) *J. Neurophysiol.* **74,** 479–483.